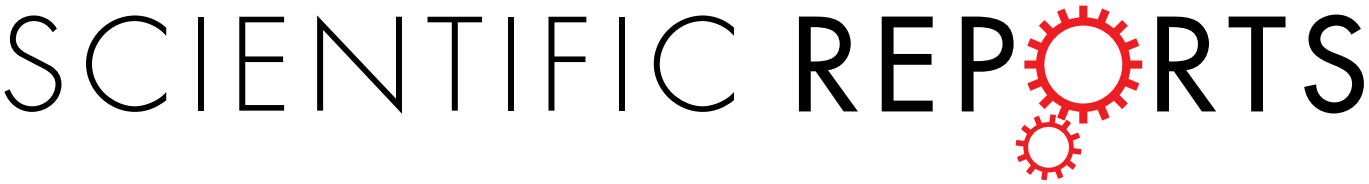

OPEN

Methyl iodine over oceans from the Arctic Ocean to the maritime Antarctic

Received: 27 January 2016
Accepted: 25 April 2016
Published: 17 May 2016

Qihou Hu[1,2], Zhouqing Xie[2], Xinming Wang[1], Juan Yu[2] & Yanli Zhang[1]

Studies about methyl iodide (CH_3I), an important atmospheric iodine species over oceans, had been conducted in some maritime regions, but the understanding of the spatial distribution of CH_3I on a global scale is still limited. In this study, we reports atmospheric CH_3I over oceans during the Chinese Arctic and Antarctic Research Expeditions. CH_3I varied considerably with the range of 0.17 to 2.9 pptv with absent of ship emission. The concentration of CH_3I generally decreased with increasing latitudes, except for higher levels in the middle latitudes of the Northern Hemisphere than in the low latitudes. For sea areas, the Norwegian Sea had the highest CH_3I concentrations with a median of 0.91 pptv, while the Central Arctic Ocean had the lowest concentrations with all values below 0.5 pptv. CH_3I concentration over oceans was affected by many parameters, including sea surface temperature, salinity, dissolved organic carbon, biogenic emissions and input from continents, with distinctive dominant factor in different regions, indicating complex biogeochemical processes of CH_3I on a global scale.

Iodine plays an important role on atmospheric chemistry by destroying tropospheric ozone and forming new particles[1–3], especially in the marine boundary layer. Among the iodine species, methyl iodide (CH_3I) with its relatively high concentration and long lifetime (~7 days) in the atmosphere is thought to be the dominate volatile organic iodine compounds (VOICs) which works as the carrier of iodine atoms from seawater to the atmosphere[4–7], although other VOICs, such as ethyl iodide (C_2H_5I), chloroiodomethane (CH_2ClI), diiodomethane (CH_2I_2) and bromoiodomethane (CH_2BrI)[8–11], as well as inorganic iodine, such as hypoiodous acid (HOI) and I_2[12], are also widely detected over oceans.

CH_3I is usually considered to be derived from oceans[13]. Emission from photochemical reactions in the surface sea water is the dominant source of CH_3I[6,13]. Biogenic activity of phytoplankton and macroalgae is also its important source[14], especially in coastal regions[15]. Besides, terrestrial ecosystems, such as rice cultivation[16,17], peatland and wetland[18], also have contribution to atmospheric CH_3I, and are even comparable to oceanic emissions in some local areas[19]. Biomass burning releases a small quantity of CH_3I, but its contribution is negligible on the global scale[20]. However, anthropologic activities like fossil fuel combustion and industrial emissions are not regards as the source of CH_3I. Because the emission of CH_3I varies with a wide range from different sources and in different regions and seasons, the estimated global flux of CH_3I has great uncertainty[21]. More observations with comprehensive spatial and seasonal scales would help reduce the uncertainty.

There have been a considerable number of studies about CH_3I over oceans or at coastal sites[22–30]. The typical concentrations of CH_3I in the marine boundary layer were 0.1–5 pptv, with higher levels over coastal areas than remote oceans[13]. Yokouchi, *et al.*[31] reported atmospheric CH_3I concentrations on a wide scale including in the high, middle, and low latitudes of the both hemispheres. Recently, through several ship-based observation, Ooki, *et al.*[32] firstly mapped CH_3I and some other VOICs in surface seawater from the Arctic to the Antarctic, especially in the Indian Ocean, Bering Sea, and western Arctic Ocean. However, the data for the spatial distribution of CH_3I in the marine boundary layer on a global scale is still limited, especially little study has been conducted over oceans in the high latitudes of the Northern Hemisphere like the central Arctic Ocean[33], where abruptly sea ice change occurs due to global warming.

[1]State Key Laboratory of Organic Geochemistry, Guangzhou Institute of Geochemistry, Chinese Academy of Sciences, Guangzhou, 510640, China. [2]Institute of Polar Environment, School of Earth and Space Sciences, University of Science and Technology of China, Hefei, 230026, China. Correspondence and requests for materials should be addressed to Z.Q.X. (email: zqxie@ustc.edu.cn)

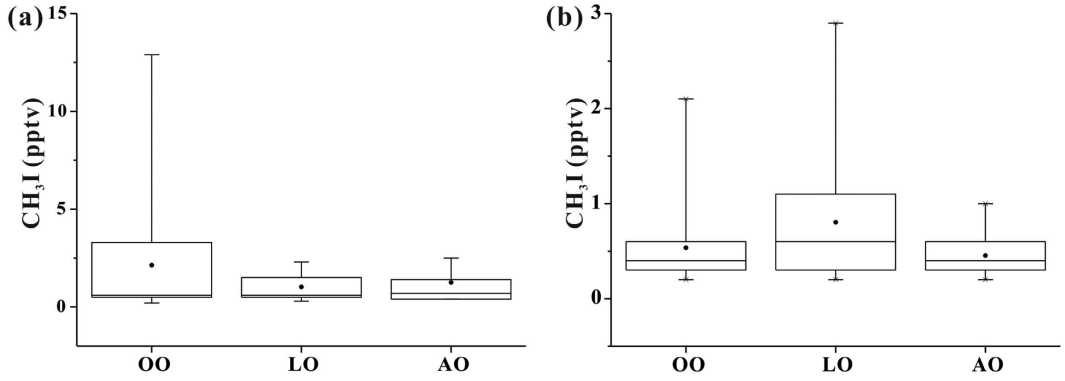

Figure 1. Box-and-whisker plots of CH_3I concentrations in ocean origin (OO), land origin (LO) and Antarctic origin (AO) samples with CO concentration (**a**) below or equal to 150 ppbv and (**b**) above 150 ppbv during the CHINARE 11/12 and the CHINARE 12. The lower and upper boundaries of the box represent the 25th and the 75th percentiles, respectively; the whiskers below and above the box indicate the minimum and maximum, respectively; the line within the box marks the median; the dot represents the mean.

During the 28th Chinese Antarctic Research Expedition (CHINARE 11/12, November 2011–April 2012) and the 5rd Chinese Arctic Research Expedition (CHINARE 12, July–September, 2012), ambient air samples were collected in the marine boundary layer from the Arctic to the Antarctic, across more than 150° latitudes, along cruise path from the Norwegian Sea through the central Arctic Ocean, the Chukchi Sea, the western North Pacific Ocean, the eastern Indian Ocean and the southern Ocean to the maritime Antarctic. The results reveals the spatial distribution of CH_3I over oceans on a global scale, as well as the potential sources and influencing factors of atmospheric CH_3I, and hence provides new constraint for the model simulating the impact of CH_3I on climate change.

Results

Potential CH_3I emission from ships. CH_3I is usually not thought to originate from anthropogenic emissions. Exceptionally, Yokouchi, *et al.*[10] found that when air mass derived from polluted continental areas, CH_3I mixing ratios at Hateruma Island in the East China Sea (24.05°N, 123.8°E) increased concurrently, indicating possible anthropogenic sources. However, other influencing factors, such as biogenic emissions from macroalgae in coastal seas or terrestrial ecosystems, cannot be eliminated. For samples in this study, CO was simultaneously determined with CH_3I. In the marine boundary layer, including over coastal regions where influenced by input from continents, the concentration of CO is usually not more than 150 ppbv[34–36]. Extremely high CO levels indicate probable pollution by ship emissions. Although the sampling site was on the foredeck of the ship and upwind from the exhaust plume, the pollution from the ship was not absolutely excluded due to diffusive emissions[37]. As presented in Table S1 in the supplementary materials, during both the CHINARE 11/12 and the CHINARE 12, the average, maximum and median mixing ratios of CH_3I in samples with CO concentration above 150 ppbv ($CO > 150$ ppbv) were much higher than those in samples with CO concentration below or equal to 150 ppbv ($CO \leq 150$ ppbv). Besides, the difference between CH_3I concentrations in samples with $CO > 150$ ppbv and those with $CO \leq 150$ ppbv during the both two cruises was significant (heteroscedastic t-test, $P < 0.05$).

In order to determine the reason for the increase of CH_3I mixing ratios in samples with $CO > 150$ ppbv, based on 7-day air mass back trajectories (BTs), we split these samples into three groups: ocean origin (OO), land origin (LO) and Antarctic origin (AO) as the same way of our previous study[38]. Air mass of OO samples only transported over oceans during the past 7 days, whereas air mass of AO and LO samples passed through continental Antarctica and other continents, respectively. The sampling sites when $CO > 150$ ppbv included both coastal regions and remote oceans (Figure S1). The mean levels of CH_3I in LO, AO and OO samples when $CO > 150$ ppbv were 1.0 ± 0.69, 1.2 ± 0.93 and 2.1 ± 3.2 pptv (mean $\pm$ standard deviation, SD, the same below), respectively (Fig. 1a). There was no significant difference (heteroscedastic t-test, $P > 0.05$) among the three groups of samples. Emissions from macroalgae in coastal regions or terrestrial ecosystems could not explain the abruptly increased CH_3I concentrations in OO samples when $CO > 150$ ppbv. Ship emission was probably caused the increase of CH_3I concentrations in OO samples. Besides, owing to the existence of iodine in fossil fuel, such as petroleum[39] and coal[40], the combustion of fossil fuel may be a potential source of atmospheric CH_3I. Direct measurement of combustion exhaust in further studies will be in favor for confirming this source.

Spatial distribution. In order to avoid the disturbance from ship emission, only samples with $CO \leq 150$ ppbv were selected to discuss the spatial distribution of CH_3I concentration during the CHINARE 11/12 and CHINARE 12 (Fig. 2, Table 1). The mixing ratios of CH_3I ranged from 0.17 to 2.9 pptv, with a mean of 0.56 ± 0.41 pptv and a median of 0.46 pptv. The mean levels of CH_3I for LO, OO and AO samples were 0.80 ± 0.61, 0.53 ± 0.37 and 0.46 ± 0.19 pptv, respectively (Fig. 1b). CH_3I concentrations in LO samples were significantly higher than those in OO and AO samples ($P < 0.05$). Emissions form macroalgaes in coastal regions can cause high CH_3I concentrations in LO samples, while low sea surface temperature (SST) and sea ice coverage may depress CH_3I production and sea-air exchange[5,41], and thus resulted in low CH_3I levels in AO samples. Saiz-Lopez, *et al.*[13] summarized mixing ratios of CH_3I in the marine boundary layer ranged as a mean level of 1.6 pptv and a median level

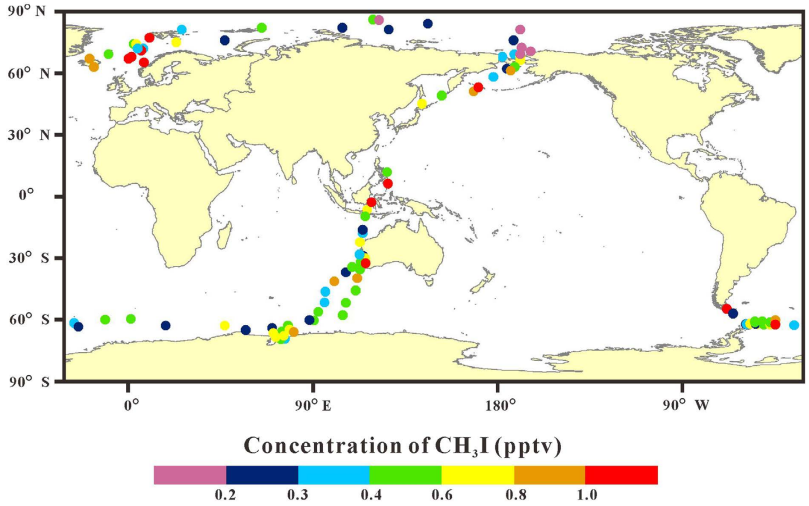

Figure 2. The spatial distribution of CH_3I concentrations in the marine boundary layer when the concentration of CO below 150 pptv during the CHINARE 11/12 and the CHINARE 12. Base map is from ArcGIS 10.0 software (http://www.esri.com).

Region	range	Mean (±SD)	median
East Antarctic	0.20–0.89	0.46 ± 0.21	0.37
West Antarctic	0.22–1.6	0.56 ± 0.38	0.42
Southern Ocean	0.24–0.95	0.51 ± 0.19	0.49
Australian adjacent Sea	0.20–1.3	0.51 ± 0.31	0.51
Southeast Asia Sea	0.49–1.4	0.90 ± 0.45	0.62
west North pacific	0.28–2.9	0.91 ± 0.83	0.74
Chukchi Sea	0.17–0.70	0.30 ± 0.19	0.22
Central Arctic Ocean	0.17–0.46	0.28 ± 0.12	0.24
Barents Sea	0.22–0.67	0.43 ± 0.23	0.39
Norwegian Sea	0.30–2.1	0.92 ± 0.52	0.91
60°S–90°S	0.20–1.6	0.48 ± 0.25	0.42
30°S–60°S	0.24–1.5	0.60 ± 0.33	0.51
30°N–30°S	0.20–1.4	0.62 ± 0.43	0.54
30°N–60°N	0.31–2.9	1.1 ± 1.0	0.80
60°N–90°N	0.17–2.1	0.56 ± 0.44	0.42
Southern Hemisphere	0.20–1.6	0.52 ± 0.29	0.46
Northern Hemisphere	0.17–2.9	0.65 ± 0.56	0.47

Table 1. Range, mean (±SD) and median of CH_3I (pptv) in different regions during the CHINARE 11/12 and the CHINARE 12.

of 1.2 pptv over coastal regions (corresponding to LO and AO samples in this study), and a mean level of 0.87 pptv and a median level of 0.70 pptv over open oceans (corresponding to OO samples in this study). It demonstrated that CH_3I mixing ratios in the marine boundary layer in 2011–2012 were relatively lower than previous observations. It may be relevant to the SST-related decadal anomalies of CH_3I emissions[30]. Similarly, in some coastal sites, such as Happo Ridge (36.7°N, 137.8°E), Hateruma Island (24.1°N, 123.8°E) and Cape Grim (40.4°S, 144.6°E), evident downtrend of CH_3I concentrations were observed from 2010[30]. It should be pointed out that CH_3I concentrations show seasonal variation, with different patterns in different latitudes[31]. In this study, due to limited observation time in each region through ship-based research, seasonal variation cannot be investigated. But the sampling time will be considered when discussing spatial distribution. Detailed results with sampling information are listed in Table S2.

CH_3I in the marine boundary layer is principally produced through photochemical reaction in the sea surface, which is affected by solar radiation intensity and dissolved organic carbon (DOC) concentration in sea surface water[5,42]. The transport of CH_3I from sea to air is controlled by SST[26,41]. Therefore, previous studies over the Pacific Ocean and Atlantic Ocean revealed obviously decreasing trend of CH_3I concentrations with increasing latitudes[29,31]. In this study, samples in the low latitudes (30°N–30°S) were collected in the spring and autumn. According to Yokouchi, *et al.*[31], no pronounced seasonal variation was observed in this region. CH_3I concentration in the low latitudes ranged from 0.20 to 1.4 pptv, with a mean of 0.62 ± 0.43 pptv and a median of 0.54 pptv.

The mean and median concentrations of CH_3I in the low latitudes were higher than those in the high latitudes (60°–90°) of both hemispheres and those in the middle latitudes (30°–60°) of the Southern Hemisphere, but they were lower than those in the middle latitudes in the Northern Hemisphere (Table 1). Previous studies also indicated that the concentration of CH_3I near the equator is slightly suppressed[31,41]. The chemical loss of CH_3I in the seawater and marine boundary layer is mainly through the nucleophilic substitution reaction with chloride (Cl^-) whose rate depends on temperature[13,43]. Thereby, although the production and emission of CH_3I in the low latitudes is the rapidest, the accumulation amount of atmospheric CH_3I may be weakened due to high loss rate. Moreover, intense convection in the tropical latitudes[44] will accelerate the dilution of CH_3I, and cause the decrease of CH_3I concentration in the boundary layer[31]. Moreover, seasonal variation of CH_3I concentration with a peak value during our sampling time in 30°–60°N is also a reason causing the lower concentrations in the low latitudes than in the middle latitudes of the Northern Hemisphere (see below).

The highest CH_3I concentrations, with the mean of 1.1 ± 1.0 pptv and the median of 0.80 pptv, were found in the middle latitudes of the Northern Hemisphere where samples were collected in the summer. In the middle latitudes, CH_3I concentrations reach the peak in the summer and early autumn and reach the tough in the winter[31]. High solar radiation and sea-surface DOC in the middle latitude in the summer can promote the photochemical emission of CH_3I[13]. Besides, most samples in the middle latitudes of the Northern Hemisphere were collected in coastal regions where the emission from large algae can further enhance CH_3I concentrations. In the western North Pacific Ocean (including the Sea of Okhotsk and the Bering Sea), CH_3I concentrations ranged from 0.28 to 2.9 pptv, with a mean of 0.91 ± 0.83 and a median 0.74 pptv, which were comparable to the results in the early-middle autumn reported by Yokouchi, *et al.*[25] and the results in the summer reported by Yokouchi, *et al.*[31] Correspondingly, CH_3I concentrations in the seawater in September–October in this region also showed high levels[32]. In the middle latitudes of the Southern Hemisphere, most samples were collected in the spring and autumn, and CH_3I concentrations were lower than those in the middle latitudes of the Northern Hemisphere, with a mean of 0.60 ± 0.33 pptv and a median of 0.51 pptv. Over the Australian adjacent Sea, CH_3I concentrations ranged from 0.20 to 1.3 pptv, with an average of 0.51 ± 0.31 pptv and a median of 0.51 pptv, which were near to the data reported by Yokouchi, *et al.*[31] at Cape Grim, a coastal site of Australia (a mean of ~0.60 pptv and a median ~0.64 pptv) in the same months (March and November). Unlike previous observation over the Southern Ocean in the summer[45], during which the peak value reached up to 2.6 pptv, CH_3I concentrations in this study ranged from 0.24 to 0.95 pptv, with a mean of 0.51 ± 0.19 pptv and a median of 0.49 pptv. Similarly, Ooki, *et al.*[32] reported that in the autumn, CH_3I concentrations in the seawater in the Southern Ocean dropped compared with those in lower latitudes.

In the high latitudes of the Northern Hemisphere and the Southern Hemisphere, samples were mostly collected in the summer, and CH_3I concentrations were in relatively low levels as a whole. The median levels in the two regions were both only 0.42 pptv. CH_3I concentrations over the Arctic Ocean, including the Chukchi Sea and the Central Arctic Ocean, stayed in very low levels (Fig. 2), with medians of 0.22 and 0.24 pptv, respectively. Accordingly, the lowest CH_3I concentrations in the seawater on a global scale were also found in the Chukchi Sea and the west part of the Central Arctic Ocean[32]. Especially, all the CH_3I concentrations over the Central Arctic Ocean were below 0.5 pptv (Table 1). Low SST (about 0 °C during our sampling in the Central Arctic Ocean) may reduce the photochemical and biogenic production of CH_3I. Moreover, sea-air exchange is also depressed by low SST and the coverage of sea ice. However, the results reported by Yokouchi, *et al.*[33] in the Chukchi Sea and the west part of the Central Arctic Ocean in the autumn were much high than our data, with a range of 0.33–0.85 pptv and a mean of 0.52 pptv. This disparity may be caused by seasonal variation. In the high latitudes of both hemispheres, CH_3I concentrations display a minimum in the summer and a maximum in the winter[31]. This seasonal pattern is caused by limited local emission throughout the year and more photolytic decomposition in the summer due to intense solar radiation in the high latitudes. Dramatically, over the Norwegian Sea, the average and median concentrations were as high as 0.92 ± 0.52 pptv and 0.91 pptv, respectively, which were higher than those over all the other seas. Although located in the high latitudes, the photochemical production rate and sea-air flux of CH_3I in the Norwegian Sea are probably in high levels, because the average SST was about 10 °C during our sampling. In addition, biogenic emission may also have an important contribution owing to high oceanic primary production in the summer in the Norwegian Sea[46]. Overall, atmospheric CH_3I concentrations in the Antarctic were relatively low, but higher than those over the Arctic Ocean. This spatial distribution pattern is also consistent with that for CH_3I in seawater[32]. The mean and median concentrations of CH_3I over the coastal region of the West Antarctic (including the Antarctic Peninsular and the Drake Passage) were slightly higher than those over the East Antarctic (Table 1). It may be caused by more oceanic emission in the West Antarctic due to higher SST in this region (2.3 °C in average) than in the East Antarctic (0 °C in average) during sampling.

Discussion

Role of sea surface temperature (SST). The concentration of CH_3I over oceans is mainly influenced by oceanic production, sea-air exchange and chemical loss in the seawater and atmosphere. Generally, high SST will promote the photochemical production of CH_3I and sea-air exchange[5,41], and thus correspond to high CH_3I mixing ratios in the marine boundary layer. However, the relationship between CH_3I concentration in the air and SST was not linear. As showed in Figure S2, atmospheric concentrations of CH_3I increased with increasing SST and reached a peak at 10–15 °C, but rapidly deceased and stay at low levels at SST of 15–30 °C, and increased with SST above 30 °C. This trend coincides well with the pattern between SST and CH_3I in the seawater reported by Ooki, *et al.*[32], that CH_3I concentrations show a peak at SST of ~15 °C and a tough at SST of ~25 °C. In the Norwegian Sea, SST ranged from 6.1 to 14 °C, and showed significantly positive correlation ($R = 0.62$, $P < 0.05$) with atmospheric CH_3I concentration (Table 2). However, in the other regions, no obvious relationship between CH_3I and SST was found. It may be due to complex influencing factors of atmospheric CH_3I other than SST. For instance,

Region	SST	WD	SSS	CDOM	isoprene	α-pinene	CO	chlorophyll-*a* exposure						
								1-day	2-day	3-day	4-day	5-day	6-day	7-day
East Antarctic	−0.39	0.28	0.06	−0.30	−0.26	−0.23	0.05	−0.12	−0.02	−0.16	−0.07	−0.10	−0.18	−0.19
West Antarctic	0.28	−0.15	**−0.57**	−0.40	−0.09	−0.19	−0.14	−0.22	0.03	0.00	−0.07	0.01	−0.11	−0.13
Southern Ocean	0.21	−0.49	0.24	−0.18	−0.02	0.22	0.03	**0.65**	0.41	0.36	0.41	−0.28	−0.26	−0.26
Australian adjacent Sea	−0.08	0.45	0.51	−0.52	−0.16	−0.27	0.09	−0.05	−0.04	0.07	−0.02	0.07	0.49	**0.67**
Southeast Asia Sea	0.45	−0.50	−0.55	−0.40	−0.83	**0.89**	−0.09	0.51	0.45	0.44	0.38	0.25	0.03	−0.14
West North pacific	−0.16	−0.04	0.40	0.04	0.30	0.42	**0.73**	0.26	0.02	−0.01	0.01	0.01	0.01	0.04
Chukchi Sea	−0.02	−0.04	−0.27	0.72	−0.23	_[a]	0.38	0.72	0.80	0.79	**0.98**	**0.99**	**0.98**	**0.96**
Central Arctic Ocean	0.28	−0.15	−0.57	−0.40	−0.09	−0.19	−0.14	−0.22	0.03	0.00	−0.07	0.01	−0.11	−0.13
Barents Sea	0.24	−0.92	0.17	−0.39	0.93	0.93	−0.14	_[b]	_[b]	_[b]	_[b]	_[b]	_[b]	_[b]
Norwegian Sea	**0.62**	0.53	−0.18	**0.71**	0.19	**0.75**	0.50	**0.65**	0.19	**0.66**	**0.70**	0.30	0.13	0.09

Table 2. Correlation coefficients of CH_3I with the sea surface temperature (SST), wind speed (WD), sea surface salinity (SSS), colored dissolved organic matter (CDOM), concentrations of isoprene, α-pinene and carbon monoxide (CO), and 1-day to 7-day chlorophyll-*a* exposure in different regions during the CHINARE 11/12 and the CHINARE 12[*]. [*]Values with $P < 0.05$ are in bold. [a]α-pinene was not detected in the Chukchi Sea. [b]Satellite chlorophyll-a data was lack in the Barents Sea during sampling.

in the Norwegian Sea, CH_3I also well correlated with colored dissolved organic matter (CDOM), which is a component of DOC and can partly reflect its level (Table 2).

Role of biogenic emission indicated by chlorophyll-a. Because CH_3I in the marine boundary layer is affected by biogenic emission, its concentration should have relativity with chlorophyll-*a*. Previous studies reveals that CH_3I does not present well correlation with *in-situ* chlorophyll-*a*, but significantly correlated with chlorophyll-*a* exposure along back trajectories over the past several days[45,47]. According to Lai, *et al.*[45], chlorophyll-a data from NASA was taken at 6-hourly position along the back trajectories to calculate chlorophyll-a exposure over 1–7 days prior to reach the sampling site. As presented in Table 2, over the Norwegian Sea, CH_3I concentration was significantly correlated with 1-day, 3-day and 4-day chlorophyll-*a* exposure, indicating that both local source and long-range transport of biogenic emissions affect CH_3I in this region. CH_3I also had significant relationship with 4-day to 7-day chlorophyll-*a* exposure in the Chukchi Sea and with 7-day chlorophyll-*a* exposure in the Australian Adjacent Sea, indicating the influence from long-range transport of biogenic emission; while significant correlation between CH_3I and 1-day chlorophyll-*a* exposure in the Southern Ocean, indicating the contribution of local biogenic emission. In the Norwegian Sea and Southeast Asian Sea, CH_3I also present significantly positive correlation with α-pinene released by phytoplankton[48] (Table 2), indicating joint sources. For instance, *prochlorococcus* is a major biogenic source of CH_3I[49], and its spatial distribution, high levels in the low and middle latitudes, also agrees with that of CH_3I. Meanwhile, *prochlorococcus* presents high α-pinene emission rate[48]. However, over the two seas, no significant relationship was found between CH_3I and isoprene, another important biogenic volatile organic compound (BVOC) species over oceans[50]. This discrepancy may be due to many other functional types of phytoplankton with high isoprene emission rate, such as *synechococcus*, *haptophytes* and diatoms species[51].

Role of sea surface salinity and other physical factors. Significantly negative correlations between CH_3I concentration and sea surface salinity (SSS) was found in the coastal region of the West Antarctic ($R = -0.57$, $P < 0.05$). Similarly, the decreasing trend of CH_3I concentration in the seawater with the increasing SSS was observed at Kiel Fjord in the Baltic Sea[52]. High SSS value means high Cl^- in the seawater, and thus causes more CH_3I depleted in the seawater. However, the parameters link to production and sea-air exchange of CH_3I, such as SST, wind speed (WD) and CDOM did not present obvious relationship with atmospheric CH_3I in the West Antarctic. It indicated that rather than emission, chemical loss dominated CH_3I concentrations in this region. Besides these factor, in the western North Pacific Ocean, dramatically, CH_3I showed significant correlation with CO ($R = 0.73$, $P < 0.05$), indicating combustion emissions. CH_3I concentrations in LO samples (0.80–2.9 pptv) were much higher than those in OO samples (0.31–0.68 pptv), further suggesting the input from continents. This region is heavily affected by biomass burning in the East Siberia[53], which can also emit CH_3I[54]. Besides, anthropogenic sources like fossil fuel burning possibly also played a role on CH_3I over oceans[10]. In the Central Arctic Ocean, the Barents Sea and the coastal region of the East Antarctic Ocean, no parameter was found to be significantly correlated with CH_3I concentration. It may be caused by the offset of the role of each factor and too low CH_3I levels in these seas.

Experimental Methods

Sampling. Ambient air samples were collected between the East China Sea to the coastal regions of Antarctica (35°N–70°S) during the CHINARE 11/12 and between the East China Sea to the Arctic Ocean (37°N–88°N) during the CHINARE 12. The sampling site located upwind on the upper-most deck of the icebreaker *Xuelong*. 2-L electro-polished stainless steel canisters, which can keep gases in it out of light and avoid photochemical reaction, were used to collect ambient air samples. Prior to the cruises, the canisters were cleaned and evacuated. Each sampling lasted for about 5 minutes. After sampling, the canisters were then stored in a dark and thermostatic

room at 4 °C during the cruises. After the cruises, samples were sent to the Guangzhou Institute of Geochemistry (GIG), Chinese Academy of Sciences, for analysis immediately. All the analysis was done within 6 months after collection for the CHINARE 11/12 samples, and within 3 months for the CHINARE 12 samples. Yokouchi, *et al.*[50] reported that CH_3I does not show significant decline in canisters 6-month after sampling.

Chemical analysis. A Model 7100 pre-concentrator (Entech Instruments Inc., California, USA) coupled with an Agilent 5973 N gas chromatography-mass selective detector/flame ionization detector (GC-MSD/FID, Agilent Technologies, USA) was used to analyse volatile organic compounds (VOCs) in the canister samples. Details of the analytical procedure were previously described[55]. Briefly, 500 mL air sample in the canister was first concentrated in a liquid-nitrogen cryogenic trap at −160 °C. Then, pure helium transferred the trapped VOCs to a secondary trap at −40 °C with Tenax-TA as an adsorbent. During these two processes, the majority of H_2O and CO_2 were removed. The secondary trap was then heated to transfer the target VOCs to a third cryo-focus trap at −170 °C by helium. The third trap was heated rapidly to transfer the VOCs into the GC-MSD/FID system. Helium was used with a HP-1 capillary column (60 m × 0.32 mm × 1.0 μm, Agilent Technologies, USA) as carrier gas and then divided in two ways: The first was a PLOT-Q column (30 m × 0.32 mm × 2.0 μm, Agilent Technologies, USA) followed by FID detection. The second was a 65 cm × 0.10 mm I.D stainless steel line followed by MSD detection. The GC oven temperature was initially set at −50 °C for 3 min and increased to 10 °C at 15 °C min^{-1}, then 120 °C at 5 °C min^{-1}, then 250 °C at 10 °C min^{-1} and remaining at 250 °C for 10 min. The MSD was used in selected ion monitoring (SIM) mode and the ionization method was electron impact ionization (EI). CH_3I concentrations were obtained from the signal of MSD. CO in the canister was separated by a packed column (5 Å Molecular Sieve 60/80 mesh, 3 m × 1/8 in.), converted to CH_4 by a Ni-based catalyst, and then analyzed by an Agilent 6890 gas chromatograph equipped with an FID.

Quality Control and Assurance. Before the cruises, all canisters were cleaned at least five times by filling and evacuating with humidified zero air. In order to check any possible contamination in the canisters, all canisters were evacuated after the cleansing procedures, re-filled with pure nitrogen, stored in the laboratory for at least 24 h, and then the same methods as field samples were used to analyse VOCs and ensure that no target compounds were found or that they were under the method detection limit. CH_3I was identified based on its retention times and mass spectra, and quantified by a mixture standard with 0.58 pptv of CH_3I in it from the Rowland/Blake laboratory at the University of California, Irvine[56]. The comparison of quantification between the GIG laboratory and the Rowland/Blake laboratory had been conducted through duplicate samples[57]. The relative measurement deviations were within 4% for CH_3I. Before sample analysis, the analytical system was checked daily with a one-point calibration. If the results were beyond ±10% of the initial calibration curve, recalibration was performed. The detection limit for CH_3I in this study is ~0.10 pptv.

Data of chlorophyll-*a*, sea ice and air mass back trajectories. Satellite chlorophyll-a data in the surface seawater were obtained by Moderate Resolution Imaging Spectroradiometer (MODIS) from NASA satellites (http://oceancolor.gsfc.nasa.gov). Air mass back trajectories (BTs) were calculated for the samples using HYSPLIT (HYbrid Single-Particle Lagrangian Integrated Trajectory) transport and dispersion model from the NOAA Air Resources Laboratory (http://www.arl.noaa.gov/ready/hysplit4.html). 7-day BTs for each sampling were traced with 6 h steps at 50 m above sea level.

References

1. Davis, D. *et al.* Potential impact of iodine on tropospheric levels of ozone and other critical oxidants. *J. Geophys. Res.* **101,** 2135–2147 (1996).
2. O'Dowd, C. D. *et al.* Marine aerosol formation from biogenic iodine emissions. *Nature* **417,** 632–636 (2002).
3. Carpenter, L. J. Iodine in the marine boundary layer. *Chem. Rev.* **103,** 4953–4962 (2003).
4. Lovelock, J. E. Natural halocarbons in air and in Sea. *Nature* **256,** 193–194 (1975).
5. Moore, R. M. & Zafiriou, O. C. Photochemical production of methyl iodide in seawater. *J. Geophys. Res.* **99,** 16415–16420 (1994).
6. Richter, U. & Wallace, D. W. Production of methyl iodide in the tropical Atlantic Ocean. *Geophys. Res. Lett.* **31,** L23S03 (2004).
7. Wang, L., Moore, R. M. & Cullen, J. J. Methyl iodide in the NW Atlantic: Spatial and seasonal variation. *J. Geophys. Res.* **114,** C07007 (2009).
8. Schall, C. & Heumann, K. G. GC determination of volatile organoiodine and organobromine compounds in Arctic seawater and air samples. *Fresen. J. Anal. Chem*. **346,** 717–722 (1993).
9. Carpenter, L. *et al.* Short-lived alkyl iodides and bromides at Mace Head, Ireland: Links to biogenic sources and halogen oxide production. *J. Geophys. Res.* **104,** 1679–1689 (1999).
10. Yokouchi, Y., Saito, T., Ooki, A. & Mukai, H. Diurnal and seasonal variations of iodocarbons (CH_2ClI, CH_2I_2, CH_3I, and C_2H_5I) in the marine atmosphere. *J. Geophys. Res.* **116,** D06301 (2011).
11. Peters, C. *et al.* Reactive and organic halogen species in three different European coastal environments. *Atmos. Chem. Phys.* **5,** 3357–3375 (2005).
12. Carpenter, L. J. *et al.* Atmospheric iodine levels influenced by sea surface emissions of inorganic iodine. *Nature Geosci.* **6,** 108–111 (2013).
13. Saiz-Lopez, A. *et al.* Atmospheric Chemistry of Iodine. *Chem. Rev.* **112,** 1773–1804 (2012).
14. Hughes, C. *et al.* The production of volatile iodocarbons by biogenic marine aggregates. *Limnol. Oceanogr.* **53,** 867–872 (2008).
15. Carpenter, L., Malin, G., Liss, P. & Küpper, F. Novel biogenic iodine-containing trihalomethanes and other short-lived halocarbons in the coastal east Atlantic. *Global Biogeochem. Cycles* **14,** 1191–1204 (2000).
16. Muramatsu, Y. & Yoshida, S. Volatilization of methyl iodide from the soil-plant system. *Atmos. Environ.* **29,** 21–25 (1995).
17. Lee-Taylor, J. & Redeker, K. Reevaluation of global emissions from rice paddies of methyl iodide and other species. *Geophys. Res. Lett.* **32,** L15801 (2005).
18. Dimmer, C. H., Simmonds, P. G., Nickless, G. & Bassford, M. R. Biogenic fluxes of halomethanes from Irish peatland ecosystems. *Atmos. Environ.* **35,** 321–330 (2001).
19. Sive, B. C. *et al.* A large terrestrial source of methyl iodide. *Geophys. Res. Lett.* **34,** L17808 (2007).
20. Blake, N. J. *et al.* Biomass burning emissions and vertical distribution of atmospheric methyl halides and other reduced carbon gases in the South Atlantic region. *J. Geophys. Res.* **101,** 24151–24164 (1996).

21. Bell, N. *et al.* Methyl iodide: Atmospheric budget and use as a tracer of marine convection in global models. *J. Geophys. Res.* **107,** 4340 (2002).
22. Singh, H. B., Salas, L. J. & Stiles, R. E. Methyl halides in and over the eastern Pacific (40°N-32°S). *J.Geophys. Res. Oceans* **88,** 3684–3690 (1983).
23. Reifenhäuser, W. & Heumann, K. G. Determinations of methyl iodide in the Antarctic atmosphere and the South Polar Sea. *Atmos. Environ.* **26,** 2905–2912 (1992).
24. Atlas, E., Pollock, W., Greenberg, J., Heidt, L. & Thompson, A. Alkyl nitrates, nonmethane hydrocarbons, and halocarbon gases over the equatorial Pacific Ocean during SAGA 3. *J. Geophys. Res.* **98,** 16933–16947 (1993).
25. Yokouchi, Y. *et al.* Distribution of methyl iodide, ethyl iodide, bromoform, and dibromomethane over the ocean (east and southeast Asian seas and the western Pacific). *J. Geophys. Res.* **102,** 8805–8809 (1997).
26. Yokouchi, Y., Nojiri, Y., Barrie, L. A., Toom-Sauntry, D. & Fujinuma, Y. Atmospheric methyl iodide: High correlation with surface seawater temperature and its implications on the sea-to-air flux. *J. Geophys. Res.* **106,** 12661–12668 (2001).
27. Cohan, D., Sturrock, G., Biazar, A. & Fraser, P. Atmospheric methyl iodide at Cape Grim, Tasmania, from AGAGE observations. *J. Atmos. Chem.* **44,** 131–150 (2003).
28. Cox, M., Sturrock, G., Fraser, P., Siems, S. & Krummel, P. Identification of regional sources of methyl bromide and methyl iodide from AGAGE observations at Cape Grim, Tasmania. *J. Atmos. Chem.* **50,** 59–77 (2005).
29. Butler, J. H. *et al.* Oceanic distributions and emissions of short-lived halocarbons. *Global Biogeochem. Cycles* **21,** GB1023 (2007).
30. Yokouchi, Y. *et al.* Long-term variation of atmospheric methyl iodide and its link to global environmental change. *Geophys. Res. Lett.* **39,** L23805 (2012).
31. Yokouchi, Y. *et al.* Global distribution and seasonal concentration change of methyl iodide in the atmosphere. *J. Geophys. Res.* **113,** D18311 (2008).
32. Ooki, A., Nomura, D., Nishino, S., Kikuchi, T. & Yokouchi, Y. A global-scale map of isoprene and volatile organic iodine in surface seawater of the Arctic, Northwest Pacific, Indian, and Southern Oceans. *J.Geophys. Res. Oceans* **120,** 4108–4128 (2015).
33. Yokouchi, Y., Inoue, J. & Toom-Sauntry, D. Distribution of natural halocarbons in marine boundary air over the Arctic Ocean. *Geophys. Res. Lett.* **40,** 4086–4091 (2013).
34. Stehr, J. *et al.* Latitudinal gradients in O_3 and CO during INDOEX 1999. *J. Geophys. Res.* **107,** 8016 (2002).
35. Sommariva, R. & von Glasow, R. Multiphase halogen chemistry in the tropical Atlantic Ocean. *Environ. Sci. Technol.* **46,** 10429–10437 (2012).
36. Großmann, K. *et al.* Iodine monoxide in the Western Pacific marine boundary layer. *Atmos. Chem. Phys.* **13,** 3363–3378 (2013).
37. Lohmann, R. *et al.* Potential contamination of shipboard air samples by diffusive emissions of PCBs and other organic pollutants: implications and solutions. *Environ. Sci. Technol.* **38,** 3965–3970 (2004).
38. Hu, Q.-H. *et al.* Secondary organic aerosols over oceans via oxidation of isoprene and monoterpenes from Arctic to Antarctic. *Sci. Rep.* **3,** 2280 (2013).
39. Tullai, S., Tubbs, L. E. & Fehn, U. Iodine extraction from petroleum for analysis of $^{1,2,9}I/^{127}I$ ratios by AMS. *Nucl. Instr. Meth. Phys. Res. B.* **29,** 383–386 (1987).
40. Germani, M. S. & Zoller, W. H. Vapor-phase concentrations of arsenic, selenium, bromine, iodine, and mercury in the stack of a coal-fired power plant. *Environ. Sci. Technol.* **22,** 1079–1085 (1988).
41. Blake, N. J. *et al.* Distribution and seasonality of selected hydrocarbons and halocarbons over the western Pacific basin during PEM-West A and PEM-West B. *J. Geophys. Res.* **102,** 28315–28331 (1997).
42. Happell, J. D. & Wallace, D. W. Methyl iodide in the Greenland/Norwegian Seas and the tropical Atlantic Ocean: Evidence for photochemical production. *Geophys. Res. Lett.* **23,** 2105–2108 (1996).
43. Elliott, S. & Rowland, F. S. Nucleophilic substitution rates and solubilities for methyl halides in seawater. *Geophys. Res. Lett.* **20,** 1043–1046 (1993).
44. Andreae, M. O. *et al.* Transport of biomass burning smoke to the upper troposphere by deep convection in the equatorial region. *Geophys. Res. Lett.* **28,** 951–954 (2001).
45. Lai, S. C. *et al.* Iodine containing species in the remote marine boundary layer: A link to oceanic phytoplankton. *Geophys. Res. Lett.* **38,** L20801 (2011).
46. Carr, M.-E. *et al.* A comparison of global estimates of marine primary production from ocean color. *Deep Sea Res. Part II* **53,** 741–770 (2006).
47. Arnold, S. *et al.* Relationships between atmospheric organic compounds and air-mass exposure to marine biology. *Environ. Chem.* **7,** 232–241 (2010).
48. Yassaa, N. *et al.* Evidence for marine production of monoterpenes. *Environ. Chem.* **5,** 391–401 (2008).
49. Smythe-Wright, D. *et al.* Methyl iodide production in the ocean: Implications for climate change. *Global Biogeochem. Cycles* **20,** GB3003 (2006).
50. Yokouchi, Y., Li, H. J., Machida, T., Aoki, S. & Akimoto, H. Isoprene in the marine boundary layer (Southeast Asian Sea, eastern Indian Ocean, and Southern Ocean): Comparison with dimethyl sulfide and bromoform. *J. Geophys. Res.* **104,** 8067–8076 (1999).
51. Shaw, S. L., Gantt, B. & Meskhidze, N. Production and emissions of marine isoprene and monoterpenes: a review. *Adv. Meteorol.* **2010,** 408696 (2010).
52. Shi, Q., Petrick, G., Quack, B., Marandino, C. & Wallace, D. Seasonal variability of methyl iodide in the Kiel Fjord. *J.Geophys. Res. Oceans* **119,** 1609–1620 (2014).
53. Hu, Q.-H., Xie, Z.-Q., Wang, X.-M., Kang, H. & Zhang, P. Levoglucosan indicates high levels of biomass burning aerosols over oceans from the Arctic to Antarctic. *Sci. Rep.* **3,** 3119 (2013).
54. Andreae, M. *et al.* Methyl halide emissions from savanna fires in southern Africa. *J. Geophys. Res.* **101,** 23603–23613 (1996).
55. Wang, X. & Wu, T. Release of isoprene and monoterpenes during the aerobic decomposition of orange wastes from laboratory incubation experiments. *Environ. Sci. Technol.* **42,** 3265–3270 (2008).
56. Simpson, I. J. *et al.* Characterization of trace gases measured over Alberta oil sands mining operations: 76 speciated C_2–C_{10} volatile organic compounds (VOCs), CO_2, CH_4, CO, NO, NO_2, NOy, O_3 and SO_2. *Atmos. Chem. Phys.* **10,** 11931–11954 (2010).
57. Zhang, Y. *et al.* Ambient CFCs and HCFC-22 observed concurrently at 84 sites in the Pearl River Delta region during the 2008–2009 grid studies. *J. Geophys. Res.* **119,** D021626 (2014).

Acknowledgements

This research was supported by grants from the National Natural Science Foundation of China (Project Nos 41176170, 41025020), the Program of China Polar Environment Investigation and Assessment (Project No. CHINARE2011–2016) and the External Cooperation Program of BIC, CAS (Grant No. 211134KYSB20130012). The authors acknowledge the NOAA Air Resources Laboratory (ARL) for making the HYSPLIT transport and dispersion model available on the Internet (http://www.arl.noaa.gov/ready.html).

Author Contributions

Z.Q.X. designed and supervised the study. Q.H.H., J.Y. and Y.L.Z. performed the experiment. Q.H.H. and Z.Q.X. wrote the manuscript. X.M.W. contributed to the discussion of results.

Additional Information

Supplementary information accompanies this paper at http://www.nature.com/srep

Competing financial interests: The authors declare no competing financial interests.

How to cite this article: Hu, Q. *et al.* Methyl iodine over oceans from the Arctic Ocean to the maritime Antarctic. *Sci. Rep.* **6**, 26007; doi: 10.1038/srep26007 (2016).